Iraqi Journal of Industrial Research, Vol. 9, No. 3 (2022)

Open Access

Iraqi Journal of Industrial Research (IJOIR)

Journal homepage: http://ijoir.gov.iq

A Review on the Friction Stir Brazing for Joining Dissimilar Materials

Akeel Dhahir Subhi

Production Engineering and Metallurgy Department, University of Technology – Iraq

Article information

Article history:
Received: August, 15, 2022
Accepted: November, 02, 2022
Available online: December, 14, 2022

Keywords:
Friction stir brazing,
Joint microstructure,
Joint strength

Corresponding Author:
Akeel Dhahir Subhi
akeel.d.subhi@uotechnology.edu.iq

DOI:
https://doi.org/10.53523/ijoirVol9I3ID265

Abstract

Friction stir brazing (FSB) is a new technology developed for its ability to join similar and dissimilar metals and alloys resulting in a joint with considerable characteristics through the use of interlayer (braze) material under the action of a pinless rotating tool and other FSB parameters. The frictional heat during FSB is responsible for the melting of the braze material between the two workpieces, while the shoulder action must be satisfactory for the extrusion of the excess braze liquid phase depending on the FSB parameters used. The parameters of FSB also have a considerable impact on the microstructure and mechanical characteristics of friction stir brazed (FSBed) joints. Sound interfacial bonding can be observed in the central zone of FSBed joints, where intermetallic compounds (IMCs) can be formed by direct diffusion among the dissimilar workpieces after extrusion of liquid phase rather than by mechanical mixing or solidification of braze material. Increasing the transverse speed at a constant rotational speed has an influence on the peak temperature, but it remarkably reduces the holding time owing to the increased cooling rate. The use of vibration in the FSB increments the fluidity of the molten braze material among the joining workpieces resulting in a more homogeneous distribution of IMCs particles. In this review article, FSB parameters, bonding mechanisms, as well as the microstructure, and mechanical properties of FSBed joints are reviewed.

1. Introduction

Dissimilar joints have gained great uses in various fields of industries including automotive, aerospace, marine and chemical. Moreover, these wide applications are increasing with the development of technologies [1]. Joining processes such as brazing [2, 3], soldering [4, 5], arc welding [6,7], laser welding [8, 9], hybrid welding [10, 11], electron beam welding [12, 13], resistance welding [14, 15], ultrasonic welding [16, 17], friction crush welding [18, 19] and other types of welding processes have been covered in literature. Arc welding processes among all these processes appear as not recommended processes for obtaining felicitous dissimilar welds such as Al-steel based on features of the arc-induced melting and hardening process such as the evolution of brittle intermetallic compounds (IMCs) [20]. Thus, other joining processes have been studied where no melting occurs for both parent metals. Furnace brazing [21, 22] and friction welding [23, 24] among joining processes have been extensively studied. Moreover, the joining temperature or time should be carefully controlled to a lower level to discourage the formation of excessively thick IMCs [25].

Furnace brazing is an industrial technique in which the entire assembly is heated to the melting point of the braze alloy and then poured into the joint before cooling. It has the ability to braze dissimilar materials, greater control over tolerances and avoidance of distortion in the finished part. On the other hand, the brazed joints require a high degree of cleanliness of the base metal. Design considerations are very important in furnace brazing of components as well as in final assembly [26, 27]. One of the major disadvantages of furnace brazing is not being able to provide joints such as the Cu/Al junction with the zinc filler due to poor wettability at a low joining temperature of the Al side, or cracking within a solidified structure where large IMCs are formed [28]. The mutual dissolution of dissimilar base metals and/or the liquid phase thickness should be reduced to prevent defect formation. These defects can be resolved by using friction stir brazing (FSB) [29].

The FSB was developed from FSW with an interlayer applied between the base materials to form the lap joint. Moreover, it is a potency process for brazing to fabricate a multi-layer composite without keyhole formation by multi-passes. The FSB provides several merits over the traditional brazing processes such as it does not require flux, shielding gas and a vacuum atmosphere. On the other hand, little energy is expended; as well as introducing some mechanical actions, such as forging and torquing, to remove the oxide layer and void defects [30].

The FSB parameters such as shoulder diameter, tool rotation and transverse speeds, interlayer material thickness and workpiece materials are remarkable in the FSB. The microstructural features of FSB joint compared to FSW joint differ due to the absence of the tool pin in the case of the FSB. Plastic deformation in the stirring area and other features such as particle dispersion and hook-type mechanical interlocking are averted in FSB. Moreover, IMCs are recognized in a layer form during FSB. It is recommended that the layer of IMCs be at the lowest value possible to obtain good quality joints. The preferable shear tensile strength can be acquired with decreasing IMC thickness, which is governed by process parameters. It is important to consider that the thickness of the workpiece may be a limit because the heat generated on the upper workpiece surface must be transmitted to the interface between the two workpieces [29, 31, 32].

This paper provides a review of the literature published in the FSB for joining dissimilar materials by focusing on the joining of Al-steel, Al-brass and Al-Cu sheets.

2. Bonding Mechanism of FSBed Joint

FSB is a process in which the pin-free tool consisting of a shoulder is applied to the surface of the upper fixed sheet. The other fixed sheet is kept at the lower side while interlayer material (braze metal) is applied in between where the sheets are in lap joint configuration. Multi-passes are required to generate more heat during FSB. The responsibility of the friction heat generated from the severe plastic deformation is to melt the braze foil between the two sheets, while the shoulder action, which can be improved by tilting the tool, should be satisfactory to extrude the excess liquid phase. It is remarkable to notice that the action of tool forging on the interface of the lap joint is an important feature of the FSB [33]. G. Huang et al [34] explained the mechanism of FSBed Al-brass joint formation in which Zn is used as an interlayer (Figure 1). The local joining temperature increments rapidly owing to the synchronized effect of frictional heat and plastic deformation by plunging the rotating tool into the upper Al sheet. The liquid of Al-Zn eutectic forms at the Al interface and extends towards the Al substrate, which has been forced into the concavities of the brass surface by forging action owing to extrusion, thus forming an intimate weld between the two lapped surfaces. Activation of Al, Cu, and Zn atoms also occurs to induce interdiffusion at the interface. G. Huang et al [34] also showed the occurrence of two types of diffusion, one is the liquid state diffusion at the Al interface and the other is the liquid-solid diffusion at the brass interface. The heat input with increasing transverse speed at a specific rotation speed decreases and consequently the holding time decreases. Therefore, the thinness of the interlayer is diminished. Also, as the welding speed increases somewhat, cracks initiate at the bonding interface owing to insufficiency of diffusion, particularly at the brass interface.

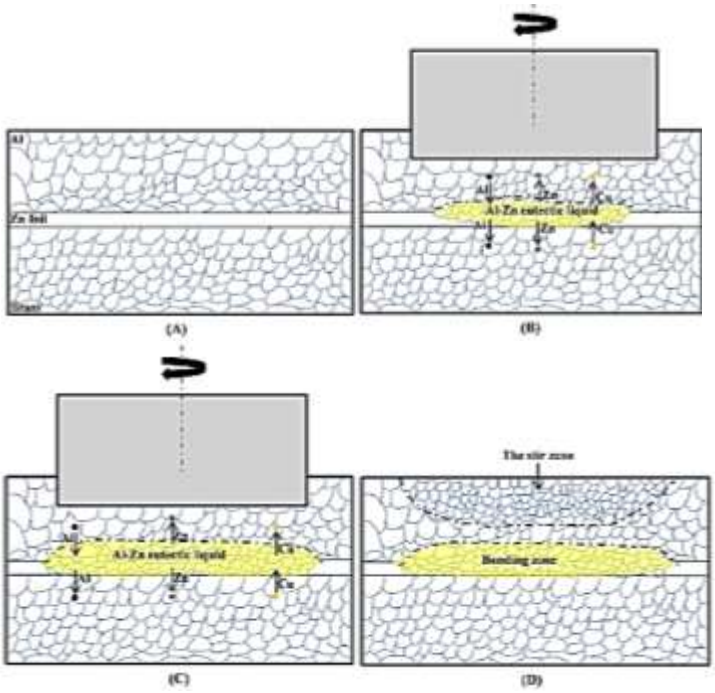

Figure (1). The mechanism of interlayer structure formation [34].

3. FSB Parameters

Various factors control the FSB process i.e., tool rotation speed, transverse speed, plunge depth, tilt angle, tool design and processing conditions. Below shows the effect of various variables in the FSB.

3.1. Transverse Speed and Tool Rotation

The two most important parameters in FSB are the transverse speed of the tool along the joint line and the second is the rotation speed of the tool in revolutions per minute (clockwise or counterclockwise). Increased tool rotation speeds cause the temperature to rise due to increased friction between the tool and the workpiece. The frictional coupling of the tool surface to the workpiece can be controlled by adjusting the parameters of the FSB and thus controlling the heat generation. The second parameter is the transverse speed, which is important because of its great influence on the thickness of the IMC layer formation which greatly affects the joint strength [29, 34, 35].

3.2. Plunge Depth

For FSB, the two lapped sheets must be clamped with the presence of an interlayer on a backing plate. The tool is plunged vertically and is rotating across the upper sheet as it moves transversely along the direction required to join the two sheets. Increasing the plunge depth of the tool increases the temperature on the advancing side (AS) and the retreating side (RS), as the joining temperature of the AS is greater than that of the RS. The difference in temperature between the AS and RS decreases as the plunge depth of the tool increases [36, 37].

3.3. Tool Tilt Angle

The tilting of the spindle towards the trailing direction at a convenient angle ensures that the tool holds the deformed material on the workpiece surface. Augmenting the tilt angle of the tool results in an increment in the temperature on the AS and the RS. The joining temperature on the AS is greater than that of the RS due to the fact that the AS is the welding side where there is a favorable combination of transverse speed and rotation speed which can increase the joining temperature. In contrast, the vector in the retreating side is in the opposite direction as it can depress the joining temperature compared to that of the AS [38, 39].

3.4. Tool Design

Tool design is the most effective in the achievement of the FSB process through its influence on the flow of the material and thus controls the transverse speed that is used during FSB. The FSB tool is made up of a shoulder without a pin, where the essential action of the tool is local heating. The heating is mainly caused in the first stage

of the tool plunging owing to the friction between the shoulder and the workpiece. Additional heating results from the deformation of the material. The largest heating component is produced from the friction between the shoulder and the workpiece. Therefore, the diameter of the shoulder is very important in terms of heating compared to other non-critical design characteristics. The other function of the shoulder is to offer a restriction on the heated volume of the material [29, 40].

4. Zones of FSBed Joint

Various distinguished microstructural zones were identified by G. Zhang et al [29] for FSBed Al-steel joint with the presence of Zn interlayer, namely, zone I (extruded Zn storage zone), zone II (transition zone), and zone III (stable zone) as shown in Figure (2).

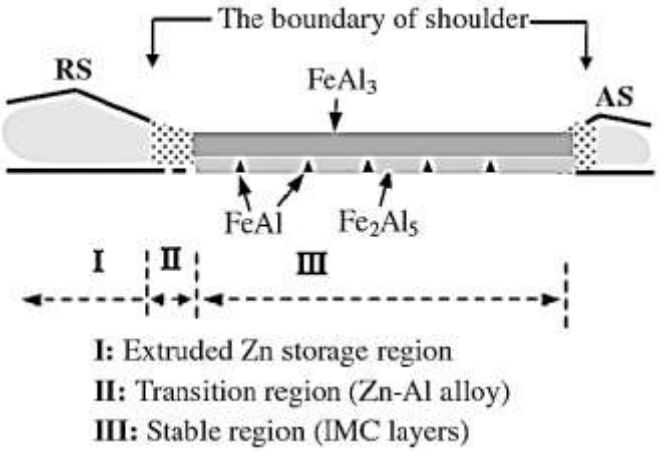

Figure (2). Cross sectional scheme of the joint by FSB [29].

In zone I (extruded zinc storage zone), there is an additional layer under the shoulder which is an extruded molten alloy including substantially of Zn and Al. This zone also includes the Al dissolution into molten Zn and excessive extrusion of molten alloy.

The interface evolution behavior is shown on the Al side in zone II. In this zone, there is an undermining of the aluminum oxide film in front of the shoulder by molten zinc in several microzones and this allows the dispersed oxide film to flow afar.

The display of interface evolution behavior can be distinguished on the steel side in zone III where partial wetting of the steel occurs by liquid Zn-Al alloy and also slightly dissolving iron as well as extrusion of molten alloys. The existence of the Zn-Al-Fe ternary eutectic reaction can further support the achievability of the slight dissolution of Fe in the Zn-Al molten alloy. The extrusion of the molten alloy including mainly Zn, Al and Fe leads to the appearance of some voids on the surface of the steel, which are removed by the forging action of the shoulder. The formation of IMC interlayers is also shown in zone III. During the forward movement of the shoulder and with enhanced heating, stirring and forging, the IMC formation is in four distinct stages. First, the initial creation of many separate IMC particles, second, the preferential joining of IMC particles along surfaces, third, ascending mixing of small IMC particles with the aid of enhanced stirring, and fourth, the rapid growth and densification of IMC layers with the aid of continual frictional heating and forging at the trailing edge of the tool. The IMC layers formation with a small amount of Zn suggests that FSB is a diffusion process instead of an in-situ solidification process.

Whereas G.F. Zhang et al [41] divided the bonding interface into five zones of FSBed Al-Cu plates in the lap configuration, as pointed out by the broken lines in Figure (3a). Zones I and V lie in the AS and RS, respectively, outside the influence of the shoulder where the interfacial region under the tool from AS to RS can be divided into three essential zones such as zone II within the AS, zone III in the center, and zone IV within RS. In zones I (outside AS) and V (outside RS), there is not pure Zn but eutectic microstructure (Figure 3b), Zn-Al-Cu alloy

(white phase in Figure 3d) or Al-Cu-Zn alloy (grey phase in Figure 3d). Considerable dissolution of both Al and Cu appears in molten Zn and the resulting liquid alloy has the ability to extrude and remove the oxide film via substrate oxide undermining and further extrusion of oxide fragments especially at the Al side using the liquid phase. Meanwhile, the initial surfaces of Al and Cu in zone V cannot be removed. The various removal behavior of oxide film in zones I (edge zone) and V (inner zone) indicates that the different thermal distribution and restriction conditions for metal flow cannot be ignored through the interfacial reaction. In zones II (inside the AS) and III (central zone), both IMCs and residual Zn are difficult to observe, indicating that excessive liquid phase extrusion, solidification cracking elimination and close contact at the joint interface are performed. However, there are few microvoids in zone II because the shoulder movement in the central region is more active compared to that in the boundary region. Simultaneously in zone IV (within the RS), interfacial bonding is accomplished on both sides of Al and Cu.

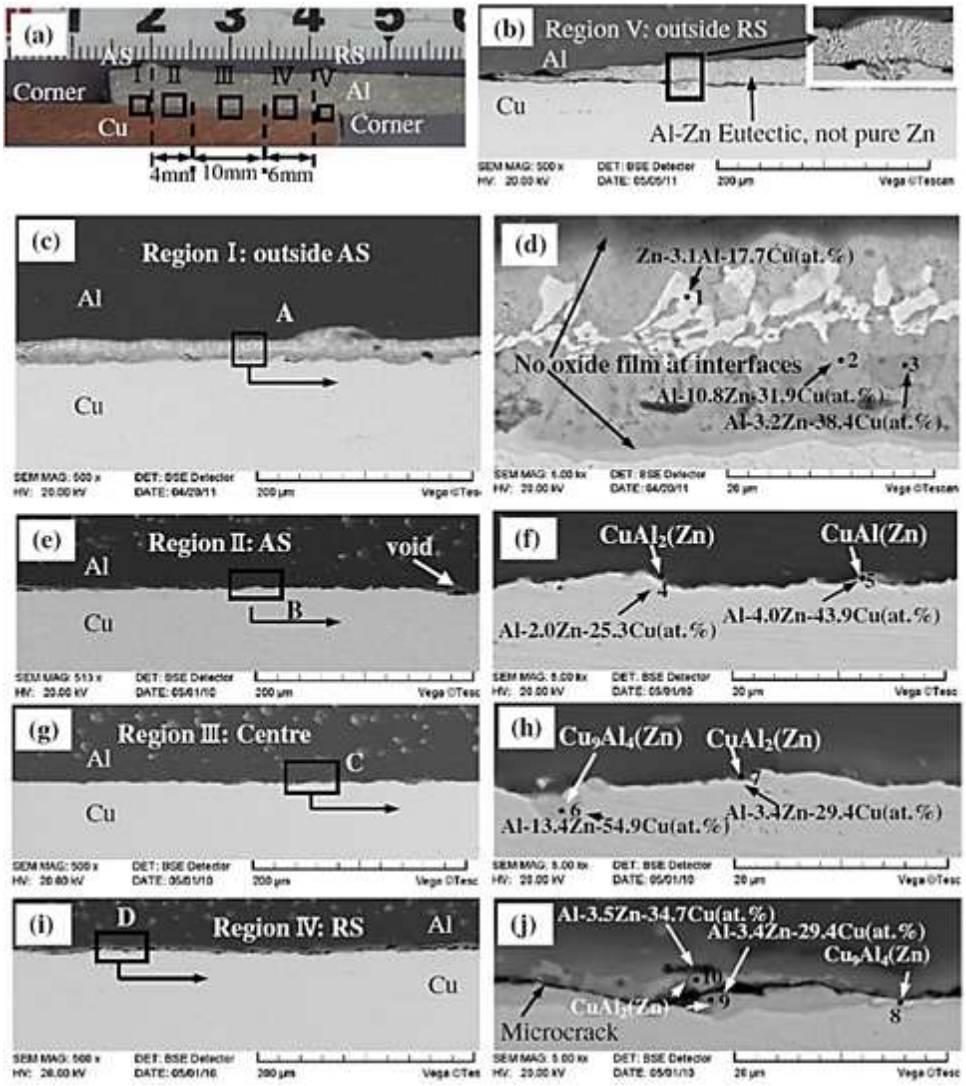

Figure (3). BSE images of FSB joint showing the different zones of FSBed joint [41].

5. Microstructural Evolution

G. Zhang et al [29] demonstrated the impact of transverse speed on the interfacial microstructure in the central region of the joint. The interface layer consists of 2 or 3 different IMC layers (Figure 4). The effects of transverse speed on the thickness of IMCs at FSBed joints can be shown in Figure (5). They observed that the thickness of the IMC tends to increase with decreasing transverse speed since when the transverse speed is 23.5 mm/min, the resulting IMC is very thick (20 µm) owing to excess heat input. Whereas for a very speedy transverse speed (eg, 300 and 375 mm/min), the evolved IMC layer is not continual and uniform along the joint interface with a low

thickness (3-5 µm) due to lack of input heat, resulting in failure to achieve intimate contact between two base metals. While for transverse speeds of 75-235 mm/min, the IMC layers formed are continual, dense and regular due to the appropriate heat input, and their thicknesses are decreased from 19-6 µm with increasing transverse speed.

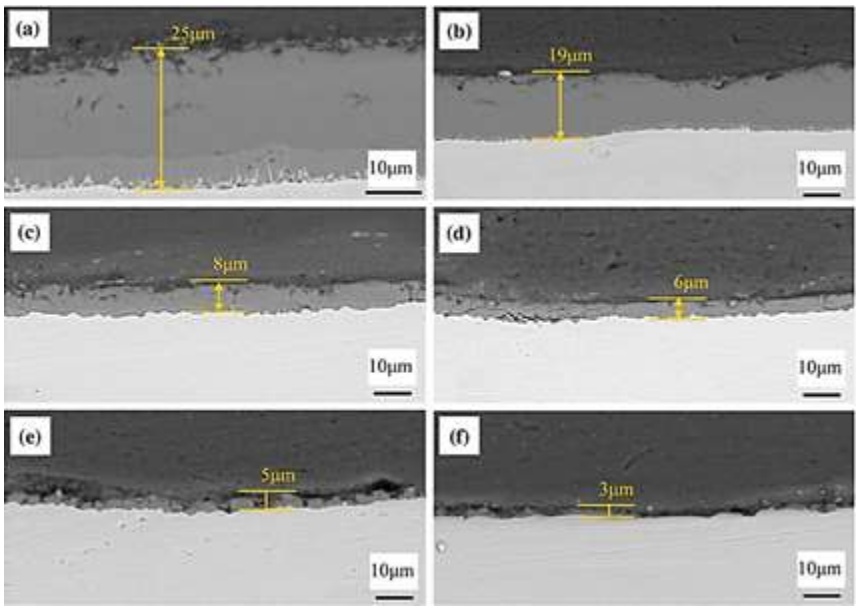

Figure (4). BSE images showing the microstructure affected by transverse speed for IMCs: (a) 23.5 mm/min, (b) 75 mm/min, (c) 150 mm/min, (d) 235 mm/min, (e) 300 mm/min, and (f) 375 mm/min [29].

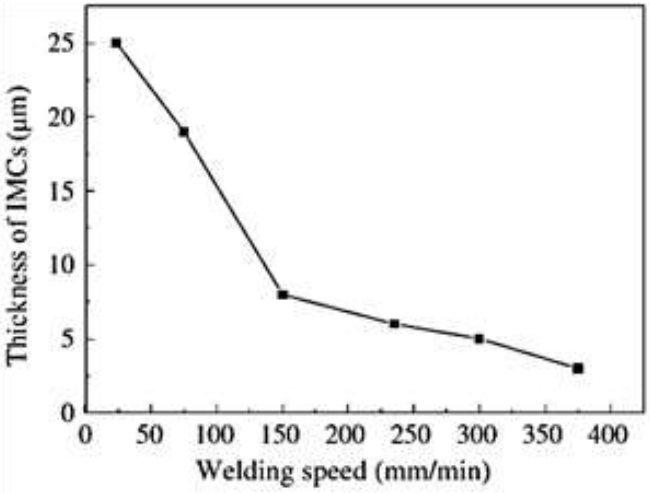

Figure (5). Thickness of IMC of FSBed joints as a function of transverse speed [29].

G. Huang et al [34] observed that there are no cracks and pores in the Al-brass joints with the Zn interlayer formed at transverse speeds of 20-60 mm/min. They showed that the thickness of the interlayer tends to decrease drastically from approximately 60 to 16 µm as the transverse speed increments from 20 to 60 mm/min due to thermal history. The over-slow transverse speed at 1800 rpm rotation speed points out higher heat input and longer holding time resulting in accelerating interlayer diffusion and therefore the interlayer resorts to thickening (Figure 6a–c). Otherwise, no sound bonding is produced to the brass substrate for the very fast transverse speed of 80 mm/min due to the diffusion being more sensitive to heat on the brass side compared to that on Al side (Figure 6d). Their findings also demonstrated the occurrence of liquid phase diffusion due to the diffusion between Al and liquid phase of Al-Zn eutectic alloy while liquid-solid diffusion is occurred due to the diffusion between the liquid phase and the brass as a result of the high melting point of brass. G. Huang et al [34] also showed that Zn-rich

particles are presented in two different places where the first is the interlayer and the second is the Al substrate close to the lap interface (Figure 6a–c). As these two types of zinc-rich particles are derived from the original zinc foil.

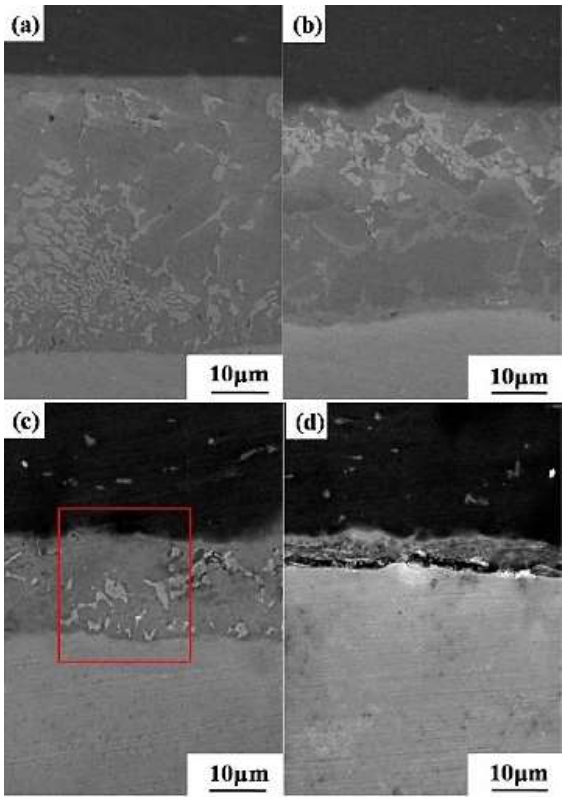

Figure (6). SEM images of Al/Zn/Br interlayer obtained by FSB using various transverse speeds: (a) 20 mm/min, (b) 40 mm/min, (c) 60 mm/min, and (d) 80 mm/min [34].

G. Zhang et al [30] showed that an IMC layer is formed in the Al-steel joint at the interface, and the Zn foil is melted completely and excelled in all the transverse speeds used (Figure 7). Whereas, for a transverse speed of 235 mm/min, which obtained the greatest joint shear strength of 55.5 MPa, a dense IMC layer of 4.7 μm thick of Al_3Fe with little zinc (<1.2 at. %) is formed in the central zone (Figure 7b). Several voids are recognized in the edge area within the IMC layer (Figure 7d), resulting in weak load bearing capacity at the edge area. The low transverse speed (150 mm/min) increments the thickness of the dense IMC layer to 6.2 μm, while the high transverse speed (375 mm/min) culminates in voids formation in the IMC layer due to lower heat input. G. Zhang et al [30] also indicated that the rotating tool is able to disrupt the IMC layer when cladding a thin Al plate on a steel surface, since the IMC is easier to disrupt than steel, and the thin upper Al plate causes stronger action of shoulder torquing on the steel surface than the thicker upper Al plate. The existence of IMC groups in Al near the interface should be favorable to reduce the thermal stress caused by the mismatch in the thermal expansion coefficient between Al and the steel.

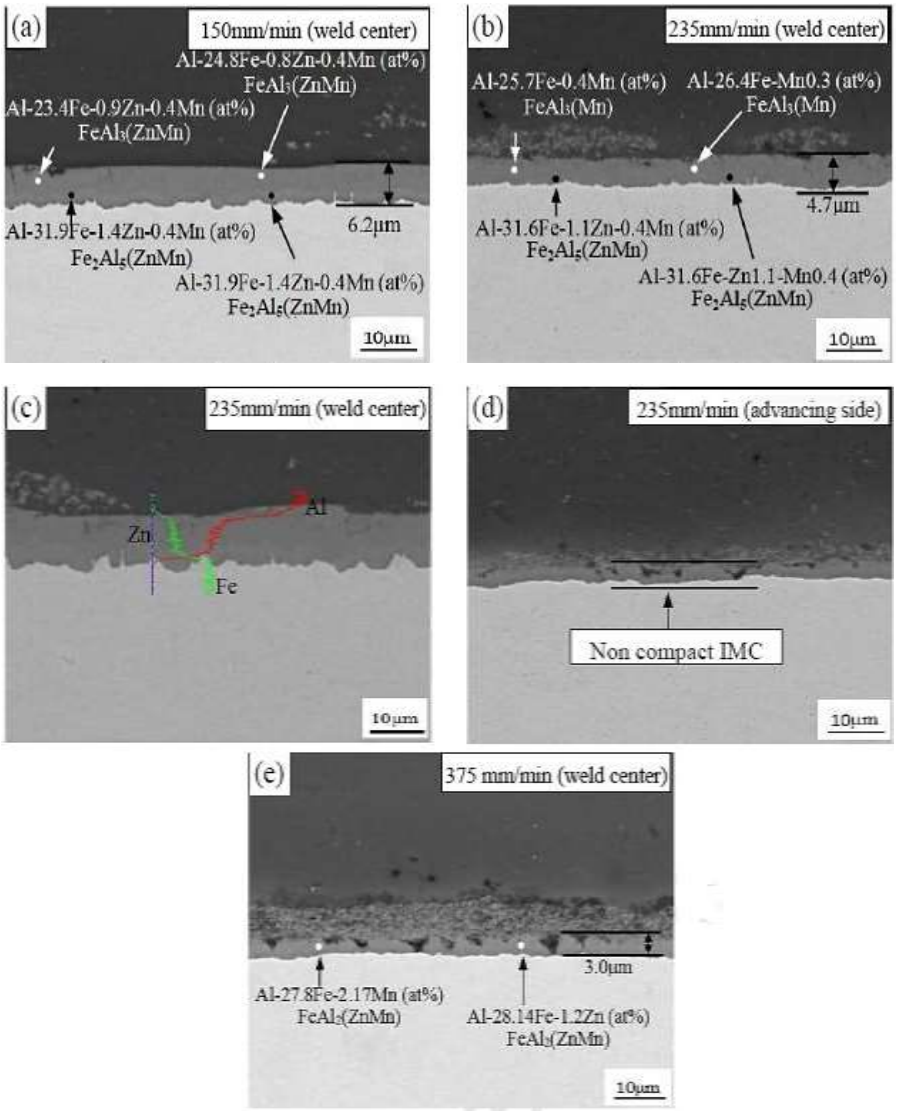

Figure (7). BSE images of the FSB pass using different transverse speeds [30].

M. Abbasi and B. Baghi [40] compare the appearance of a joint made by two brazing methods; FSB and friction stir vibration brazing (FSVB) (Figure 8a). They showed that the joint made by FSVB is smoother and has a more conventional appearance than the joint made by FSB. In addition, various flashes are recognized around the joint made by the FSB. They also demonstrated that the maximum temperature during FSVB (~245 ℃) is greater than that during FSB (~197 ℃) due to more intense friction that drives to an enhancement in the melt motility of the filler and no lack of diffusion, thus improving the chemical reaction between the base metal and the filler (Figure 8b). According to the overall structures of the joint cross-section for various conditions (Figure 8c), porosity and a lack of a coherent interface are presented in the FSBed samples, but for all the FSVBed samples, the joints with no porosity due to the effect of vibration which mechanically disrupt the oxide film on the substrate surfaces are recognized. The grain size of the FSVBed samples is smaller than that of the FSBed samples (Figure 8d). Moreover, the vibration increments the convection in the melt through nucleation and drives to a disturbance that makes waves on the metal's surfaces. Thus, the nucleation rate and quenching homogeneity will increment and as a result, the grain size will diminish.

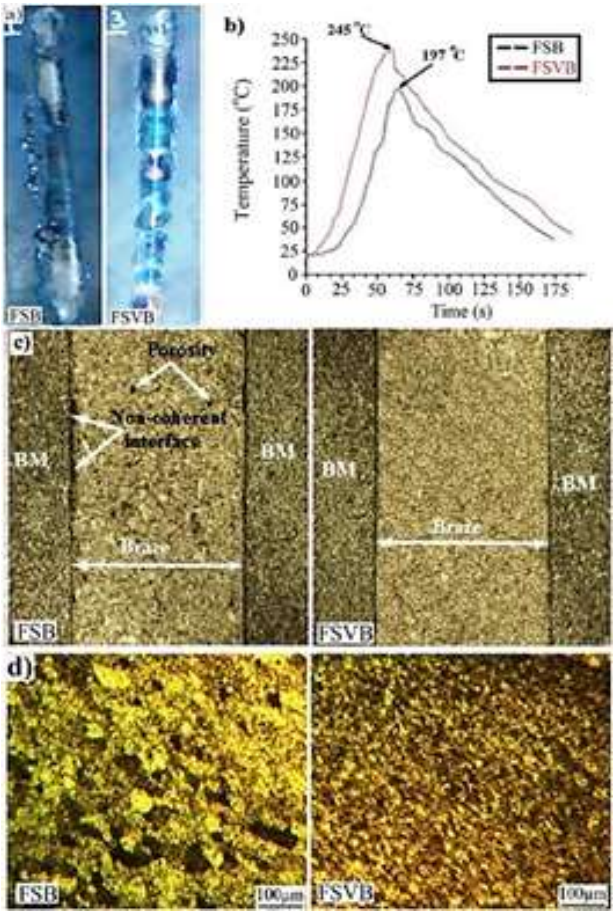

Figure (8). (a) FSBed sample, (b) Temperature distribution, (c) Joint microstructure, and (d) Brazing metal microstructure [40].

M. Abbasi and B. Baghei [40] also showed that under the influence of vibration and stirring, the filler material and IMCs are compressed in the joint area and further element distribution occurs. Thus, the brazing region is more chemically homogeneous and a thin, continual layer of IMCs is presented in the brazing region. The thickness of the IMCs of the FSBed samples is greater than that of the FSVBed samples (Figure 9a & b), where the adequate thickness of this layer improves mechanical performance. The IMC layer is broken by the action of mechanical vibration into fine particles that disperse in the joint area.

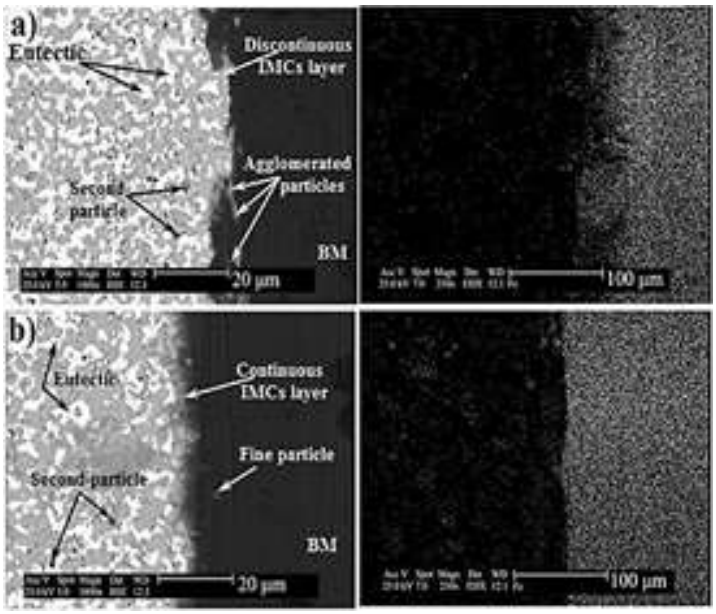

Figure (9). Interfacial microstructure of brazed specimens for (a) FSB, and (b) FSVB [40].

6. Mechanical Properties

G.F. Zhang et al [41] investigated the impact of the overlap thickness of the Al plate on the failure load (Figure 10). They showed that the failure load is decreased at the more than 2.5 mm overlap thickness of the Al plate due to the reduced width of the central area free of micro-cracks.

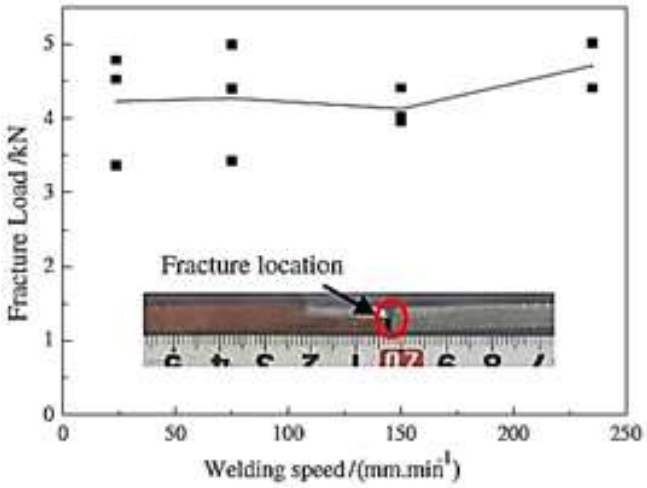

Figure (10). Fracture load versus welding speed for Al plate [41].

Shear test results of the samples with various transverse speeds were studied by G. Huang et al [34] as shown in Figure (11). They concluded that the transverse speed has a considerable influence on the failure load of the lap joint at a rotation speed of 1800 rpm. When the transverse speed is incremented from 20 to 80 mm/min at a rotation speed of 1800 rpm, the failure load is first incremented to the highest value, and then rapidly decreased. The highest failure load is achieved at transverse and rotation speeds of 60 mm/min and 1800 rpm, respectively, up to 7.62 kN, indicating that Al and brass sheets can be efficiently joined with the aid of zinc foil. The variance of failure load with transverse speed can be related to various heat generation and holding time that are affected by the change of transverse speed. They also showed that joint strength is controlled by IMC interlayer thickness and IMC types that are affected by heat generation and holding time. Augmenting the transverse speed without changing the rotation speed points out a reduction in heat input and a decrease in holding time resulting in a suppression of atomic diffusion. At a lower transverse speed (20 and 40 mm/min), more heat input and longer

holding time are offered for diffusion reactions at the lap interface resulting in increased interlayer thickness. Unfortunately, increasing the thickness will improve the brittleness of the IMC layers leading to a deterioration in the strength of the joint. However, at a higher transverse speed (80 mm/min), cracks are presented in the interface area owing to the reduction of heat input and diffusion time.

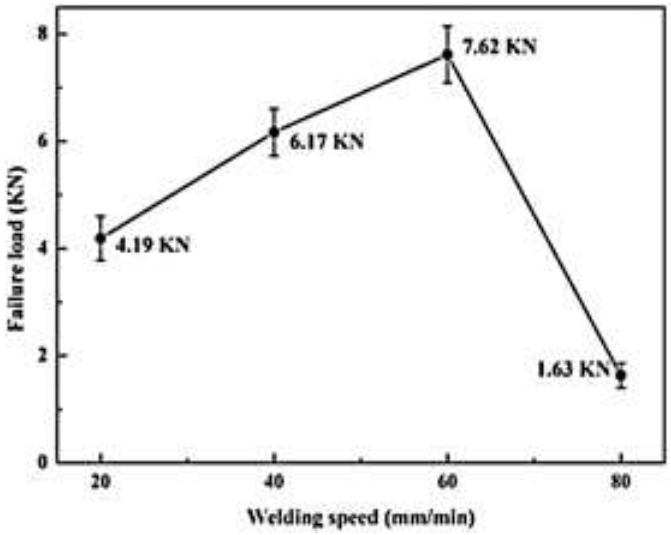

Figure (11). Shear test results of the FSBed specimens acquired using various welding speeds [34].

Y. Zhou et al [42] observed that the shear strength of Cu/Al joints increments and then decreases with augmenting shoulder diameter (Figure 12). Where the highest value of shear strength (18.67 MPa) is reported in a sample using a shoulder diameter of 12 mm, which is fractured in the heat affected zone for Al plates (Figure 12b). The lowest strength (8 MPa) is also observed in a sample using a shoulder diameter of 7 mm. The fracture surface of Cu is covered with grey substance, but there is little substance on the sample surface using a shoulder diameter of 7 mm, indicating that the interlayers are the source of the tensile failure (Figure 13). The other feature is the semicircular markings on the fracture surface of the sample using a shoulder diameter of 12 mm (Figure 13c). The torquing action is improved owing to the severe deformation under the larger shoulder, which caused the liquid metal to completely mix in the interlayer.

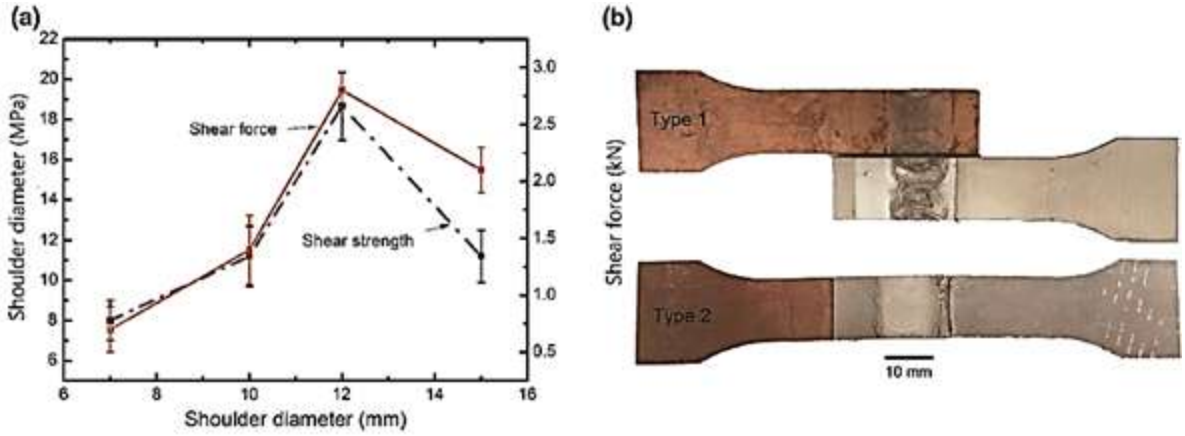

Figure (12). (a) Tensile test results and (b) images of the two fracture types [42].

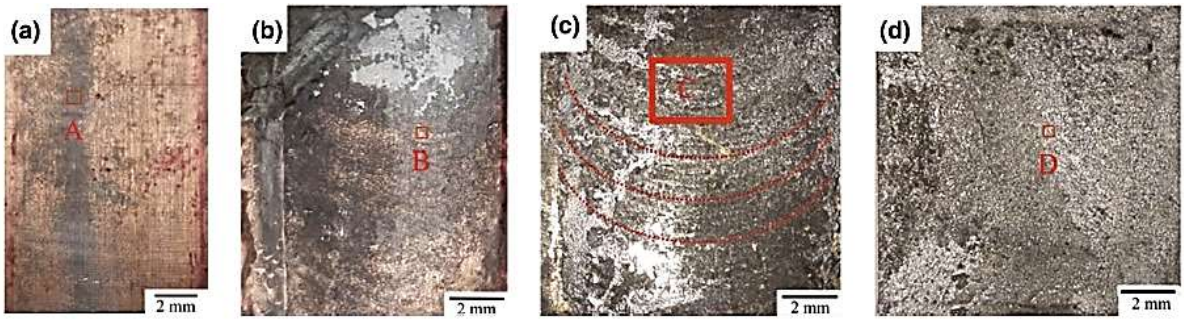

Figure (13). Images of the fracture surface Cu side for various shoulder diameters: (a) 7 mm, (b) 10 mm, (c) 12 mm, and (d) 15 mm [42].

The compressive shear test was performed by G. Zhang et al [30] to assess the pass of the FSB. They found that the preferred shear strength of 45 ~ 55 MPa can be acquired using the transverse speeds of 150-375 mm/min (Figure 14). Examination of the fracture surface indicates that the joint fractures mostly within the Al sheet, rather than along the interface in the shear test (Figure 15). The sound bonding is essentially located in the central region, while the weak bonding region is located at the edge portions. Both the shear strength and the presence of Al adhered to the sheared fracture surface of the steel confirm that the FSB process has a strong ability to clad1060Al thin sheets (as an interlayer) on strong steel even at wide transverse speeds (150 ~ 375 mm/min).

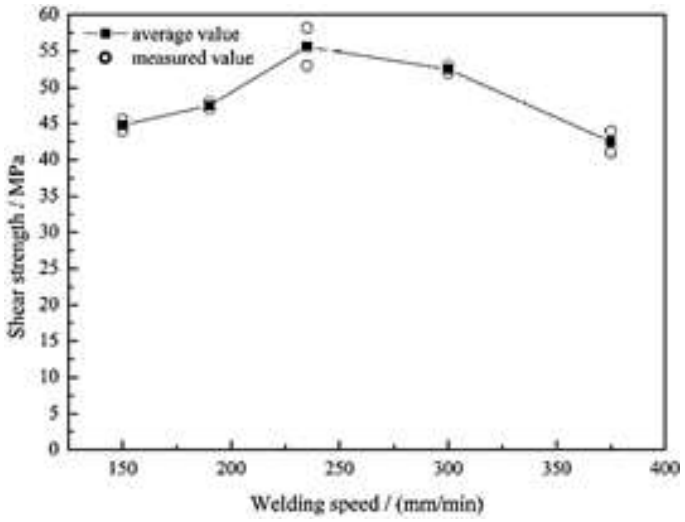

Figure (14). Compressive shear strength of the 1060Al-thin clad interlayer on 16Mn steel [30].

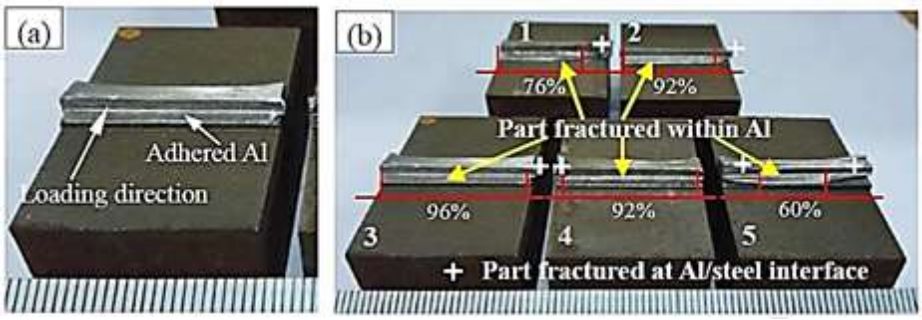

Figure (15). Fracture path of the 1060Al/steel clad joints produced using FSB pass at various transverse speeds after shear test: (a) 235 mm/min, (b) Joints collection: (1) 150 mm/min, (2) 190 mm/min, (3) 235 mm/min, (4) 300 mm/min, and (5) 375 mm/min [30].

Shear test results of copper samples joined using FSB and FSVB were demonstrated by M. Abbasi and B. Baghi [40] as shown in (Figure 16a). They showed that reducing the grain size according to the Hall-Petch relationship using FSVB results in an improvement in the volume fraction of the grain boundaries which in turn hinders the dislocation movement and as a result, the strength of the material improves. They also showed that the hardness of the brazed samples improves with the application of vibration (Figure 16b).

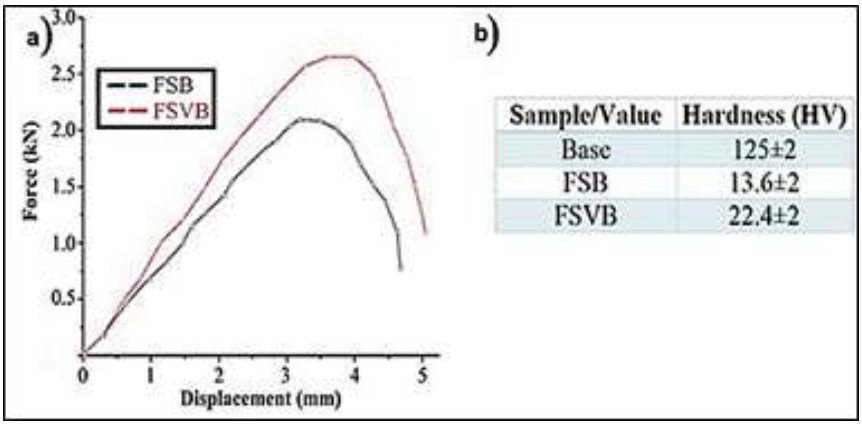

Figure (16). Results of (a) shear and (b) hardness tests [40].

7. Conclusions

It is clear that the literature indicates that the cylindrical shoulder is widely used as a joining tool. Controlling FSB parameters such as tool rotation speed, transverse speed, spindle inclination angle, and plunge depth are essential for a defectless sound joint. Two clean metal sheets can be easily joined to each other in the form of lap joints configuration. It is widely accepted that material deformation within the joint during FSB is very complex and still needs understanding. The FSB results in a significant temperature rise within the joint. Several different zones have been identified in FSB joint, i.e., zone I (extruded Zn storage zone), zone II (transition zone), and zone III (stable zone (IMC interfacial layers)). Moreover, the shear stress results of the FSBed alloys indicate that the failure commonly occurs within the heat-affected zone.

References

[1] K. Martinsen, S.J. Hu, and B.E. Carlson, "Joining of dissimilar materials", *CIRP Annals*, vol. 64, p. 679-699, 2015

[2] B. Zhang, Z. Sun, L. Zhang, D. Li, Q. Chang, and H. Pan, "Understanding the microstructure evolution mechanism and the microstructure-strength correlations of Ti_3SiC_2/Ti_2AlNb joint brazed with AgCu interlayer", *Materials Science and Engineering: A*, vol. 847, p. 143323, 2022.

[3] S. Herzog, G. Boussinot, A. Kaletsch, M. Apel, and C. Broeckmann, "Microstructure coarsening in Ba0.5Sr0.5Co0.8Fe0.2O3-δ during reactive air brazing", *Journal of the European Ceramic Society*, vol. 42, p. 5842-5850, 2022.

[4] C. Xiong, Y. Xiao, J. Zhang, D. Luo, and R. Goodall, "Microstructure transformation and mechanical properties of Al alloy joints soldered with Ni-Cu foam/Sn-3.0Ag-0.5Cu (SAC305) composite solder", *Journal of Alloys and Compounds*, vol. 922, p. 166135, 2022.

[5] H. Tatsumi, S. Kaneshita, Y. Kida, Y. Sato, M. Tsukamoto, *et al.*, "Highly efficient soldering of Sn-Ag-Cu solder joints using blue laser", *Journal of Manufacturing Processes*, vol. 82, p. 700-707, 2022.

[6] N. Muthukumaran, G Kathiresan, M.N. Shree Raam, G. Chandru, *et al.*, "Comparative studies on weldability and mechanical characteristics of semi- killed steel using different arc welding technique", *Materials Today: Proceedings*, vol. 62, p. 5471-5476, 2022.

[7] Y. Miao, Z. Wang, J. Liu, Y. Wu, *et al.*, "Effects of bypass-current and outer plasma current on the arc stability and melt pool behaviors during plasma-MIG hybrid arc welding", *Journal of Manufacturing Processes*, vol. 82, p. 415-424, 2022.

[8] M. Zhang, J. Wu, C. Mao, B. Cheng, H.M.D. Shakhawat, *et al.*, "Impact of power modulation on weld appearance and mechanical properties during laser welding of AZ31B magnesium alloy", *Optics & Laser Technology*, vol. 156, p. 108490, 2022.

[9] M. Afshari, F. Taher, M.R. Samadi, and M. Ayaz, "Optimizing the mechanical properties of weld joint in laser welding of GTD-111 superalloy and AISI 4340 steel", *Optics & Laser Technology*, vol. 156, p.108537, 2022.
[10] B. Skowrońska, J. Szulc, M. Bober, M. Baranowski, and T. Chmielewski, "Selected properties of RAMOR 500 steel welded joints by hybrid PTA-MAG", *Journal of Advanced Joining Processes*, vol. 5, p. 100111, 2022.
[11] X. Qi, P. Huan, X. Wang, X. Shen, Z. Liu, and H. Di, "Effect of microstructure homogeneity on the impact fracture mechanism of X100 pipeline steel laser-MAG hybrid welds with an alternating magnetic field", *Materials Science and Engineering: A*, vol. 851, p. 143656, 2022.
[12] K. Han, H. Wang, B. Zhang, J. Zhao, J. Lei, and X. Zhao, "Microstructural/mechanical characterizations of electron beam welded IN738LC joint after post-weld heat treatment", *Journal of Materials Research and Technology*, vol. 17, p. 1030-1042, 2022.
[13] X. Wang, H. Wang, Y. Qiu, S. Yu, *et al.*, "Formability behavior, microstructural evolution, and mechanical properties of GH4169 and electroformed Ni electron beam welded joint", *Vacuum*, vol. 204, p. 111379, 2022.
[14] Y. Yang, Y. Li, J. Bi, H. Liu, S. Ao, and Z. Luo, "Microstructure and mechanical properties of 2195/5A06 dissimilar joints made by resistance spot welding", *Materials Characterization*, vol. 191, p. 112147, 2022.
[15] U. Shah, X. Liu, A. Benatar, A. Kuprienko, and W. Zhang, "Computational analysis of the ultrasonic effects on resistance spot welding process", *Journal of Manufacturing Processes*, vol. 81, p. 191-201, 2022.
[16] J. Liu, B. Cao, and J. Yang, "Texture and intermetallic compounds of the Cu/Al dissimilar joints by high power ultrasonic welding", *Journal of Manufacturing Processes*, vol. 76, p. 34-45, 2022.
[17] N.M. Jasmin, K.A.S. Lewise, D. Raguraman, M. Murugan, *et al.*, "An overview on characteristics and performance of ultrasonic welding process on different materials", *Materials Today: Proceedings*, vol. 50, p. 1508-1510, 2022.
[18] A.S. Jomah, A.D. Subhi, and F.A. Hashim, "Effect of friction crush welding parameters on the properties of welded joints of C1020 copper sheet", Journal of Physics: Conference Series, vol. 1973, p. 012048, 2021.
[19] A.S. Jomah, A.D. Subhi, and F.A. Hashim, "Properties of welded copper tubes fabricated via friction crush welding", *Engineering and Technology Journal*, vol. 40, p. 1-10, 2022.
[20] M.M. Atabaki, M. Nikodinovski, P. Chenier, J. Ma, M. Harooni, and R. Kovacevic, "Welding of aluminum alloys to steels: An overview", *Journal for Manufacturing Science and Production*, vol. 14, p. 59-78, 2014.
[21] M. Roulin, J. W. Luster, G. Karadeniz, A. Mortensen, and A. Mortensen, "Strength and structure of furnace-brazed joints between aluminum and stainless steel", *Welding Research Supplement*, vol. 78, p. 151-s-155-s, 1999.
[22] J.B.R. Teja, K.P. Kalyan, R.V. Vignesh, and M. Govindaraju, "Vacuum brazing of mild steel using eutectic CuSil brazing alloy", *Materials Today: Proceedings*, vol. 46, p. 4919-4924, 2021.
[23] M. Zhang, Y.D. Wang, P. Xue, H. Zhang, D.R. Ni, K.S. Wang, and Z.Y. Ma, "High-quality dissimilar friction stir welding of Al to steel with no contacting between tool and steel plate", *Materials Characterization*, vol. 191, p. 112128, 2022.
[24] A. Banerjee, M. Ntovas, L. Da Silva, and S. Rahimi, "Microstructure and mechanical properties of dissimilar inertia friction welded 316L stainless steel to A516 ferritic steel for potential applications in nuclear reactors", *Manufacturing Letters*, vol. 33, p. 33-37, 2022.
[25] M.M. Abd Elnabi, T.A. Osman, A. El Mokadem, and A.B. Elshalakany, "Evaluation of the formation of intermetallic compounds at the intermixing lines and in the nugget of dissimilar steel/aluminum friction stir welds", *Journal of Materials Research and Technology*, vol. 9, p. 10209-10222, 2020.
[26] R.V Steward, M.L Grossbeck, B.A Chin, H.A Aglan, and Y Gan, "Furnace brazing type 304 stainless steel to vanadium alloy (V–5Cr–5Ti)", *Journal of Nuclear Materials*, vol. 283–287, p. 1224-1228, 2000.
[27] A. Khorram, and M. Ghoreishi, "Comparative study on laser brazing and furnace brazing of Inconel 718 alloys with silver based filler metal", *Optics & Laser Technology*, vol. 68, p. 165-174, 2015.
[28] A. Sharma, S.H. Lee, H.O. Ban, Y.S. Shin, and J.P. Jung, "Effect of various factors on the brazed joint properties in Al brazing technology", *Journal of Welding and Joining*, vol. 34, p. 30-35, 2016.
[29] G. Zhang, W. Su, J. Zhang, and Z. Wei, "Friction stir brazing: a novel process for fabricating Al/Steel layered composite and for dissimilar joining of Al to steel", *Metallurgical and Materials Transactions A*, vol. 42, p. 2850-2861, 2011.
[30] G. Zhang, X. Yang, D. Zhu, and L. Zhang, "Cladding thick Al plate onto strong steel substrate using a novel process of multilayer-friction stir brazing (ML-FSB)", *Materials & Design*, vol. 185, p. 108232, 2020.
[31] K. Mehta, "A review on friction-based joining of dissimilar aluminum-steel joints", *Journal of Materials*

Research, vol. 34, p. 78-96, 2019.
[32] J.V. Christy, A.H.I. Mourad, M.M. Sherif, and B. Shivamurthy, "Review of recent trends in friction stir welding process of aluminum alloys and aluminum metal matrix composites", *Transactions of Nonferrous Metals Society of China*, vol. 31, p. 3281-3309, 2021.
[33] M. Abbasi, B. Bagheri, F. Sharifi, and A. Abdollahzadeh, "Friction stir vibration brazing (FSVB): an improved version of friction stir brazing", *Weld World*, vol. 65, p. 2207-2220, 2021.
[34] G. Huang, X. Feng, Y. Shen, Q. Zheng, and P. Zhao, "Friction stir brazing of 6061 aluminum alloy and H62 brass: Evaluation of microstructure, mechanical and fracture behavior", *Materials & Design*, vol. 99, p. 403-411, 2016.
[35] K. Chen, X. Liu, and J. Ni, "A review of friction stir-based processes for joining dissimilar materials", *The International Journal of Advanced Manufacturing Technology*, vol. 104, p. 1709-1731, 2019.
[36] K.P. Mehta, and V.J. Badheka, "A Review on Dissimilar Friction Stir Welding of Copper to Aluminum: Process, Properties, and Variants", *Materials and Manufacturing Processes*, vol. 31, p. 233-254, 2016.
[37] G.K. Padhy, C.S. Wu, and S. Gao, "Friction stir based welding and processing technologies - processes, parameters, microstructures and applications: A review", *Journal of Materials Science & Technology*, vol. 34, p. 1-38, 2018.
[38] M.K. Kulekci, U. Esme, and B. Buldum, "Critical analysis of friction stir-based manufacturing processes", *The International Journal of Advanced Manufacturing Technology*, vol. 85, p. 1687-1712, 2016.
[39] S. Chupradit, D.O. Bokov, W. Suksatan, M. Landowski, D. Fydrych, *et al*., "Pin angle thermal effects on friction stir welding of AA5058 aluminum alloy: CFD simulation and experimental validation", *Materials*, vol. 14, p. 7565, 2021.
[40] M. Abbasi, and B. Baghei, "New attempt to improve friction stir brazing", *Materials Letters*, vol. 304, p. 130688, 2021.
[41] G.F. Zhang, K. Zhang, Y. Guo, and J.X. Zhang, "A comparative study of friction stir brazing and furnace brazing of dissimilar metal Al and Cu plates", *Metallography, Microstructure, and Analysis*, vol. 3, p. 272-280, 2014.
[42] Y. Zhou, S. Chen, D. Wang, R. Li, B. Liu, J. Pu, and Z. Yang, "Effect of shoulder diameter on the force generation, microstructure and mechanical properties of friction stir-brazed aluminium alloy and copper with ultrahigh rotation speed", *Acta Metallurgica Sinica (English Letters)*, vol. 33, p. 154-164, 2020.